Investigating tumour heterogeneity in a melanoma arising in congenital melanocytic nevus using in situ spatial gene expression analysis

Melanoma is one of the most aggressive skin cancers with high mortality rates.[1] It frequently exhibits high heterogeneity, with diverse genetic and phenotypic characteristics, which often complicate accurate diagnosis, classification and treatment planning.[2] A previous study showed that melanoma tumours with high heterogeneity tend to exhibit reduced infiltration of antitumour immune cells, lower expression of immunomodulatory genes and poorer survival.[3]

Single-cell RNA sequencing has emerged as a powerful technology for investigating melanoma cell heterogeneity and identifying subpopulations with distinct gene expression profiles; however, it lacks spatial resolution and cannot capture the positional context of cells within tissue samples.[4 5] Alternatively, spatial gene expression technologies enable the direct labelling of hundreds to thousands of transcripts within tissue sections. However, their application to skin tissue remains challenging due to the dense, fibrous dermal stroma and layered architecture of the epidermis, not to mention high intrinsic autofluorescence from melanin and other endogenous fluorophores that may interfere with imaging-based readouts.[6]

Here, we implement an in situ spatial gene expression method, Xenium (10x Genomics, Pleasanton, CA), to investigate cellular heterogeneity within a congenital melanocytic nevus (CMN). A woman in her 90s with diabetes, hypertension and dyslipidaemia presented with a 3-month history of a progressively enlarging mass on her back. A biopsy confirmed malignant melanoma arising in a CMN (Breslow thickness 3.0 mm, Clark level III, ulcerated, mitotic rate 10–15 per mm^2) without angiolymphatic or perineural invasion. Genetic analysis using a multi-target next-generation sequencing panel on a Formalin-Fixed Paraffin-Embedded (FFPE) tissue identified a *BRAF* mutation. A wide local excision and sentinel node biopsy were performed, showing no residual melanoma and negative sentinel nodes (0/2). CT imaging showed no distant metastasis, and the patient was therefore diagnosed with stage IIB melanoma (pT3bN0M0, AJCC 8th edition). We performed spatial gene expression analysis of the FFPE tissue section (DV200=72.61%) from the patient described above with the predesigned 'Human Skin' panel (260 targeted genes) using the Xenium In Situ platform. Additionally, H&E staining was also conducted on the post-Xenium slide (figure 1A). Data were generated from the on-instrument Xenium Onboard Analysis (XOA) pipeline, and we observed a total of 502,626 cells detected and 80,004,559 transcripts (Q score≥20), with a median of 139 transcripts per cell. In the XOA pipeline, before performing downstream analysis, including clustering and differential expression, cells with zero transcript counts were filtered (see full 'Materials and methods' section in online supplemental material).

The sample obtained from the patient described above represents a melanoma arising within a CMN. Histopathologic examination with H&E staining confirmed that the lesion contains both malignant melanoma (left) and benign melanocytic nevus (right) components (figure 1A). The CMN component showed bland-looking melanocytes with vertical cytologic maturation and no mitosis, whereas the melanoma component exhibited densely packed, atypical and pleomorphic melanocytes with some mitotic figures. Cells with similar expression profiles were hierarchically clustered into 10 clusters with unique expression patterns using K-means clustering method implemented in the

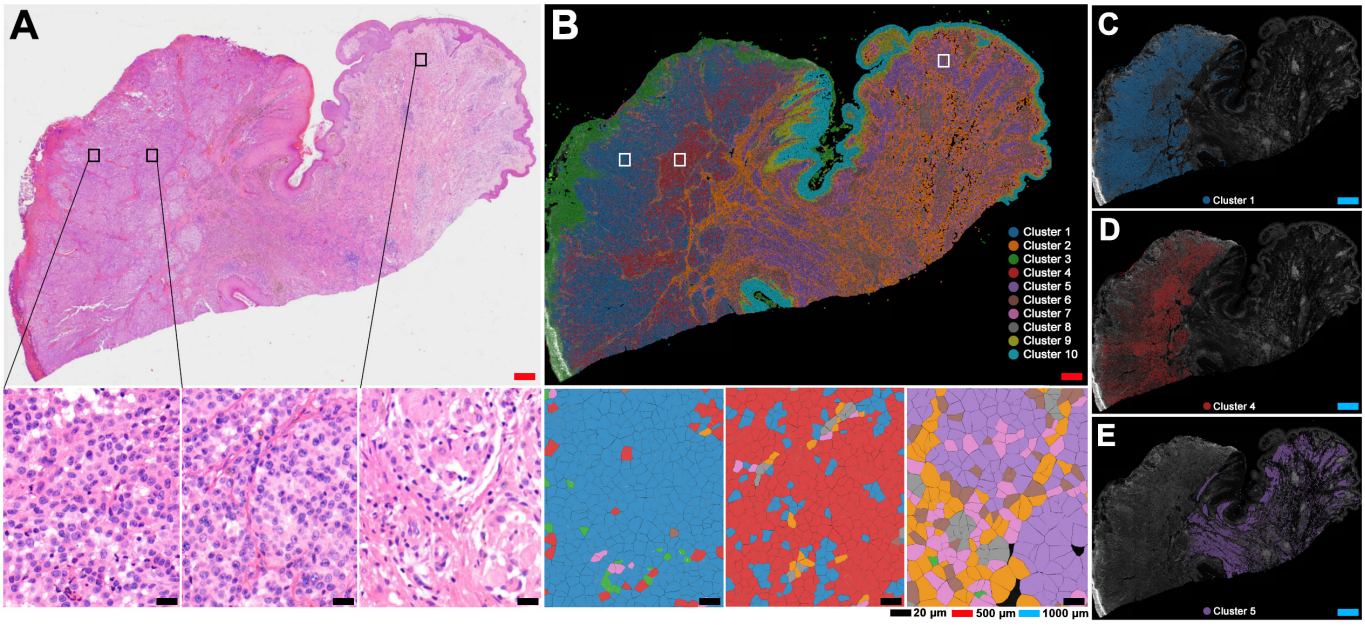

Figure 1 In situ spatial gene expression analysis showing 10 cell clusters with distinct gene expression patterns and revealed heterogeneity of the melanoma sample. (A) Post-Xenium H&E-stained image of the melanoma skin cancer tissue section with insets of higher power views of different tissue areas, namely the non-proliferative melanoma, proliferative melanoma and nevus zones. (B) Spatial visualisation of 10 clusters on the Xenium image using K-means clustering (K=10) using the Xenium Onboard Analysis pipeline. White boxes indicate the same regions as shown in (A). Spatial distribution of cells in cluster 1 (C, shown in blue), cluster 4 (D, red) and cluster 5 (E, purple). Each dot represents a cell, and the colours in the tissue section represent the different cell clusters (clusters 1–10).

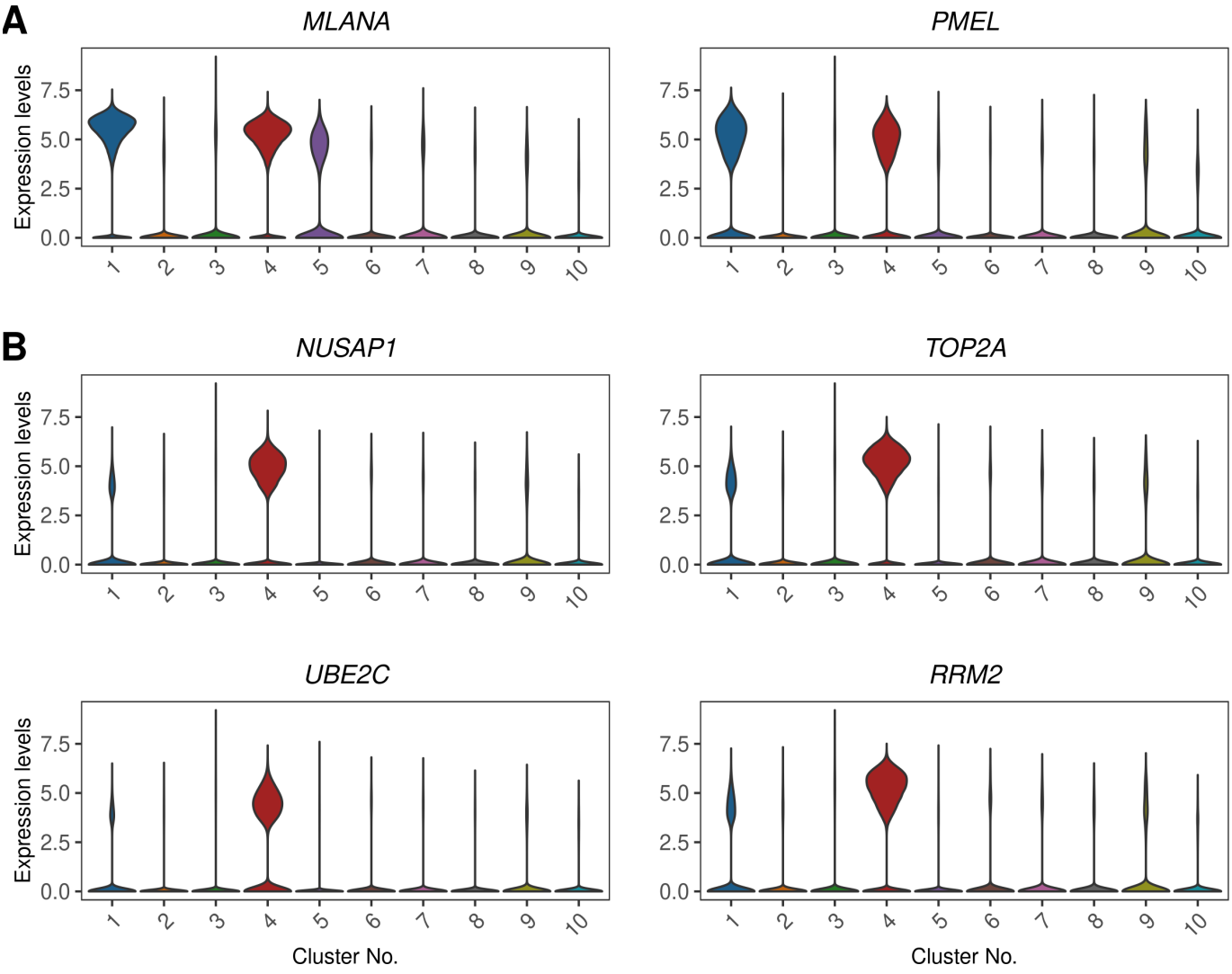

Figure 2 Expression levels of selected marker genes of melanoma and cell cycle. (A) The violin plots showing the expression levels of melanoma-associated marker genes, namely *MLANA* and *PMEL*, which were mainly seen in clusters 1 and 4. (B) The expression levels of cell cycle-associated genes, namely *NUSAP1*, *TOP2A*, *UBE2C* and *RRM2*, which were most prominent in cluster 4 but also seen to a lesser extent in cluster 1. The log-normalised transcript counts were calculated by dividing the transcript counts of a gene by total transcript counts in a cell and multiplying by scale factor (default=1000). The normalised values were then natural-log transformed. The colours of violin plots represent the different cell clusters as in figure 1B.

XOA, as shown in figure 1B. The spatial gene expression analysis can differentiate between benign and malignant melanoma regions, as shown in three different groups of cell clusters (figure 1C–E). Notably, the malignant region consisted of two cell clusters with clearly distinct expression patterns (figure 1C, D).

To determine the characteristics of each cell cluster, we further explored the differentially expressed genes between clusters and investigated the gene functions. Interestingly, the top five highly expressed genes in cluster 1, located beneath the ulcer, are *C11orf96*, *TRPM1*, *PMEL*, *MLANA* and *PLP1* (see online supplemental file and figure 2A). The presence of melanocytic markers, *PMEL* and *MLANA*, confirms that the cells in this cluster are predominantly melanoma.[7] In cluster 4, located beneath cluster 1, the top five highly expressed genes compared with other cells in the tissue sample are *NUSAP1*, *TOP2A*, *UBE2C*, *RRM2* and *TYMS* (see online supplemental file). These genes, which are associated with cell cycle regulation, DNA replication and repair functions, showed significantly higher expression levels than those observed in cluster 1 (figure 2B).[8–11] Additionally, we found that the expression of *MKI67* (marker of proliferation Ki-67)[7] was also elevated in cluster 4 (online supplemental figure 1). Expectedly, the melanoma-associated genes, *MLANA* and *PMEL*, were also highly expressed at similar levels as in cluster 1 (figure 2A). Notably, *MLANA* was also expressed in cluster 5 (figure 2A), which is regularly distributed in the CMN as well as in the melanoma part. In accordance with this finding, immunohistochemical (IHC) results using the markers HMB-45, Melan-A and Ki-67 showed that the benign melanocytic nevus exhibited markedly lower staining intensity than the melanoma (online supplemental figure 2). These findings suggest that the melanoma cells in clusters 1 and 4 represent distinct stages, with cluster 4 likely corresponding to a proliferating state, as high expression levels of cell cycle-associated genes were seen specifically in cluster 4 melanoma cells (figure 2B). Cluster 1 also mainly consists of melanoma cells; however, more likely in a senescent state, as melanoma-associated marker genes are highly expressed at similar levels

(figure 2A), whereas only a small number of cells exhibit expression of cell cycle-associated genes (figure 2B and online supplemental figure 1).

In this exploratory single-patient study, we use spatial transcriptomic technology to illustrate intratumoural gene expression heterogeneity in melanoma arising from a CMN. We have shown that conventional H&E and IHC staining alone cannot distinguish malignant lesions with heterogeneous gene expression, whereas spatial analysis revealed distinct subpopulations based on a combination of melanocytic, cell cycle, DNA replication and repair genes. These findings highlight the importance of assessing cellular heterogeneity to better understand melanoma development and identify potential biomarkers for diagnosis and treatment. However, this study was based on a single patient and a limited pre-designed 'Human Skin' panel of 260 target genes. Further studies with larger cohorts and larger gene panels will be essential to validate and extend these observations. Overall, this work demonstrates the potential of single-cell spatial gene expression imaging to uncover molecular differences between benign and malignant lesions, as well as intratumoural heterogeneity within melanoma, beyond what is detectable by standard histopathology.

Jutapak Jenkitkonchai,[1,2,3,4] **Kittiporn Punuch,**[3,5] **Teerapat Paringkarn,**[6] **Teerapat Wannawittayapa,**[6] **Manop Pithukpakorn,**[3,5] **Panitta Sitthinamsuwan,**[7] **Manasmon Chairatchaneeboon,**[6] **Varodom Charoensawan**[1,2,3,4]

[1]Division of Medical Bioinformatics, Research Department, Faculty of Medicine Siriraj Hospital, Mahidol University, Bangkok, Thailand
[2]Department of Biochemistry, Faculty of Medicine Siriraj Hospital, Mahidol University, Bangkok, Thailand
[3]Siriraj Genomics, Faculty of Medicine Siriraj Hospital, Mahidol University, Bangkok, Thailand
[4]Integrative Computational BioScience (ICBS) center, Mahidol University, Nakhon Pathom, Thailand
[5]Department of Medicine, Faculty of Medicine Siriraj Hospital, Mahidol University, Bangkok, Thailand
[6]Department of Dermatology, Faculty of Medicine Siriraj Hospital, Mahidol University, Bangkok, Thailand
[7]Department of Pathology, Faculty of Medicine Siriraj Hospital, Mahidol University, Bangkok, Thailand

Correspondence to Dr Varodom Charoensawan; varodom.cha@mahidol.ac.thDr Manasmon Chairatchaneeboon; manasmon.c@gmail.com and Dr Panitta Sitthinamsuwan; panitta.sit@gmail.com

Handling editor Vikram Deshpande.

Acknowledgements We thank Sean Tan from 10x Genomics and his team for their exceptional technical assistance and providing comprehensive training in Singapore on the 10x Xenium In Situ technology.

Contributors JJ and KP contributed equally to this paper. VC, MP, MC and PS are responsible for the conception, design and overall supervision of the study. TP, TW, MC and PS reviewed the patient charts and clinical data. KP and JJ performed the experiments. JJ performed computational analysis and visualisation. JJ, KP and VC wrote the first draft of the manuscript. All the authors reviewed, edited and approved the final version of the manuscript. VC is the guarantor. During the preparation of this work, the authors used ChatGPT and Google Gemini exclusively to improve readability and for grammar check. After using these tools, the authors reviewed and edited the content as needed and took full responsibility for the content of the publication.

Funding This study received technical and partial financial support from 10x Genomics (California, USA) and Bio-Active Co., Ltd. (Bangkok, Thailand) (for the access to the Xenium In Situ instrument and related consumables). VC is funded by the mid-career researcher grant from National Research Council of Thailand and Mahidol University (grant number N42A670557), and the Health Systems Research Institute (HSRI) of Thailand (grant number HSRI 68-063).

Disclaimer 10x Genomics and Bio-Active Co., Ltd. had no role in the study design, data interpretation and preparation of the manuscript.

Patient consent for publication Not applicable.

Ethics approval This study was conducted with ethical approval from Siriraj Institutional Review Board (COA no. Si 251/2024), Human Research Protection Unit, Faculty of Medicine Siriraj Hospital, Mahidol University.

Provenance and peer review Not commissioned; internally peer reviewed.

Data availability statement The data generated and the codes used in this study are available from the corresponding authors on reasonable request.

► Additional supplemental material is published online only. To view, please visit the journal online (https://doi.org/10.1136/jcp-2025-210509).

JJ and KP contributed equally.

To cite Jenkitkonchai J, Punuch K, Paringkarn T, *et al*. *J Clin Pathol* Epub ahead of print: [*please include* Day Month Year]. doi:10.1136/jcp-2025-210509

Received 12 November 2025
Accepted 24 November 2025

J Clin Pathol 2025;**0**:1–3.
doi:10.1136/jcp-2025-210509

ORCID iD
Varodom Charoensawan https://orcid.org/0000-0002-2199-4126

REFERENCES

1 Naik PP. Cutaneous Malignant Melanoma: A Review of Early Diagnosis and Management. *World J Oncol* 2021;12:7–19.
2 Rambow F, Marine JC, Goding CR. Melanoma plasticity and phenotypic diversity: therapeutic barriers and opportunities. *Genes Dev* 2019;33:1295–318.
3 Lin Z, Meng X, Wen J, *et al*. Intratumor Heterogeneity Correlates With Reduced Immune Activity and Worse Survival in Melanoma Patients. *Front Oncol* 2020;10:596493.
4 Ennen M, Keime C, Kobi D, *et al*. Single-cell gene expression signatures reveal melanoma cell heterogeneity. *Oncogene* 2015;34:3251–63.
5 Lim SY, Rizos H. Single-cell RNA sequencing in melanoma: what have we learned so far? *EBioMedicine* 2024;100:104969.
6 Vu T, Vallmitjana A, Gu J, *et al*. Spatial transcriptomics using combinatorial fluorescence spectral and lifetime encoding, imaging and analysis. *Nat Commun* 2022;13:169.
7 Weinstein D, Leininger J, Hamby C, *et al*. Diagnostic and prognostic biomarkers in melanoma. *J Clin Aesthet Dermatol* 2014;7:13–24.
8 Liu G, Zhao J, Pan B, *et al*. UBE2C overexpression in melanoma and its essential role in G2/M transition. *J Cancer* 2019;10:2176–84.
9 Nielsen CF, Zhang T, Barisic M, *et al*. Topoisomerase IIα is essential for maintenance of mitotic chromosome structure. *Proc Natl Acad Sci U S A* 2020;117:12131–42.
10 Raemaekers T, Ribbeck K, Beaudouin J, *et al*. NuSAP, a novel microtubule-associated protein involved in mitotic spindle organization. *J Cell Biol* 2003;162:1017–29.
11 Whitfield ML, Sherlock G, Saldanha AJ, *et al*. Identification of genes periodically expressed in the human cell cycle and their expression in tumors. *Mol Biol Cell* 2002;13:1977–2000.